Disentangling the environmental signals recorded in Holocene calcite varves based on modern lake observations and annual sedimentary processes in Diss Mere, England.

Laura Boyall[1*], José Ignacio Valcárcel[1], Poppy Harding[2], Armand Hernández[3] and Celia Martin-Puertas[1*]

[1] Department of Geography. Royal Holloway University of London. TW20 0EX Egham, Surrey, UK.

[2] Geography, Planning and Environment, Department of Psychology, Sport and Geography, University of Hertfordshire, Hatfield, Hertfordshire, AL10 9AB, UK.

[3] Universidade da Coruña, GRICA group, Centro Interdisciplinar de Química e Bioloxía (CICA), Rúa As Carballeiras, 15071 A Coruña, (Spain).

Corresponding authors:

Laura.Boyall.2016@live.rhul.ac.uk

Celia.MartinPuertas@rhul.ac.uk

Key Words

Lake monitoring, Calcite varves, Modern analogue, Lake seasonality, Palaeolimnology.

Abstract

Diss Mere is a small natural lake located in the centre of the town Diss in Norfolk (England). The lake, which has been exposed to different stressors including climate variability and changing land use, has significant recreational, historical, and environmental value. The Diss Mere sediments are annually-laminated for most of the Holocene (2.1 – 10.3 ka BP), which allows the study of the lake evolution and its response to changing environmental conditions at an exceptionally high resolution. As with many mid-latitude, alkaline lakes, Diss Mere's sediments are formed of biogenic-calcite varves. We have conducted a 3.5-year lake monitoring survey including sediment trapping to identify the main drivers and seasonal processes contributing to lake sedimentation. Our results demonstrate that the modern lake is still producing seasonally-differentiated sediments today, however, are unable to be preserved as varves due to the permanent oxygenation of the lake bottom through gradual lake shallowing. Seasonal sediment fluxes follow a general pattern of i) an early spring diatom bloom ii) spring precipitation of medium-coarse calcite grains; iii) summer precipitation of smaller endogenic calcite grains; and iv) an autumn algal bloom and endogenic calcite precipitation intermixed with benthic diatoms and micrite. Whilst calcite precipitates throughout the whole year, peaks are observed in the epilimnion during the summer. This study shows that a modern analogue approach can be applied to the varves revealing their potential for environmental and climate reconstruction and highlights the significance of monitoring surveys for modern analogue approaches to palaeolimnological research.

Introduction

Palaeoenvironmental and palaeoclimate research based on annually laminated (varved) lacustrine and marine records has increased over the last few decades. When well preserved, varved records can provide robust chronologies and have yielded evidence for past environments at very high temporal resolutions. Such records have been applied to reconstruct, for example, the frequency and magnitude of extreme weather events (Czymzik et al. 2016; Corella et al. 2014), abrupt climate changes (Brauer et al. 2008; Martin-Puertas et al. 2012), decadal climate variability (Lapointe et al. 2020; 2021), ecological responses to changing climate (Lücke and Brauer, 2004) and interactions between humans and environments (Dräger et al. 2017, Sear et al. 2020).

Advantages of lacustrine varves as a palaeoenvironmental archive is that they are globally distributed and preserve high-resolution (seasonal to annual) palaeoenvironmental information. Palaeoenvironmental proxies require careful interpretation as archives act as filters between external environmental variables such as climate, and proxies themselves. In lacustrine settings, this is termed the hydroclimate filter (Cohen et al. 2003). The hydroclimate filter integrates the physical, chemical, and biological processes in lakes, which control and modify the climate and environmental signal recorded in the sediments. Thus, the environmental and climatic interpretation of lacustrine proxies requires both an understanding of the lake system and its catchment (Sturm and Lotter, 1995), and cross-validation with other indicators from the same record through a multi-proxy approach. Based on the composition and structure of laminations, varves are commonly sorted into three types: clastic, organic, and evaporitic varves, according to conceptual models based on general lake response to seasonality in different climatic regions; cold, temperate, and (semi) arid climates, respectively (Zolitschka et al., 2015 and references therein). However, the annual nature of the laminations

and the seasonal succession of layers need validation for each individual lake. The most common practice is microscopic analysis of the laminations to identify seasonally cyclic events, such as monospecific diatom blooms, layers of authigenic mineral precipitation, or detrital deposits associated with spring snow melt and increased discharge into the catchment (Brauer et al., 2004). In lakes where varves are preserved at present, it is possible to compare sediments deposited at the lake/sediment interface with observational data of the modern limnology and sediment trapping, providing a deeper understanding of the complex interactions between the internal lake processes controlling the sediment flux (Tylmann et al., 2011; Ojala et al., 2013; Żarczyński et al., 2022). This modern analogue approach provides new insights into varve formation and the calibration of the proxy record from varved sediments (Trapote et al., 2018; Vegas-Villarrubia et al., 2020; Żarczyński et al., 2022). Special emphasis has been put on the study of biogenic-calcite varves, the most common varve type preserved in temperate, alkaline lakes. Although only a few study cases have been published (Tylmann et al. 2011; Bonk et al. 2015; Kienel et al. 2017; Trapote et al. 2018; Apolinarska et al. 2020; Roeser et al. 2021; Zander et al. 2021; Żarczyński et al. 2022), they all provide evidence of a more differentiated view of the classic light calcite/dark organic couplet reflecting the complexity of the biogeochemical annual lake cycle. This emphasises the need to better connect varve formation, the annual limnological cycle, and the external environmental conditions.

One example of a biogenic-calcite varved record is Diss Mere, UK. This site holds the only lake record in the UK published to date that preserves a continuous varved sequence through most of the Holocene from 2.1 – 10.3 ka BP (Martin-Puertas et al. 2021). From 2.1 ka BP at 9 m of sediment depth, varves stop preserving and the sediment record experienced a huge increase in sedimentation rate from 0.4 mm yr^{-1} to 5 mm yr^{-1} (Martin-Puertas et al. 2021). The end of the varved sequence is diffuse and laminations fade out over the last four varves.

The uppermost 9 m of sediments are characterised by massive deposits intercalated by ~1.5 m-thick deposits of fairly-preserved 0.5 cm-thick laminations at 7-6.3 m, 5.5-3.8 m and 2.4-1 m of sediment depth (Martin-Puertas et al., 2021). The laminations might have an annual origin according to the sedimentation rate (Yang et al., 2010; Martin-Puertas et al., 2021), which suggests that the environmental and limnological processes triggering the varve formation in the past may still be controlling the lake sedimentation today but varve preservation conditions are unfavourable and changing through time. This study reports the findings of a 3.5-year lake monitoring survey, including 4 spring-summer, and 3 autumn-winter seasons in Diss Mere, in an attempt to apply a modern analogue approach to the palaeolimnological study of this lake. Our main objectives are to: i) describe the annual lake cycle and identify the environmental processes governing the seasonality of the modern limnology and sedimentation; ii) confirm whether the seasonal material deposited today resembles the composition of the varve sub-layers in the past; and iii) discuss factors limiting varve preservation.

Study site and sediment accumulation process

Regional settings of the modern lake

Diss Mere (52º22'N, 1º6'E, 29 m a.s.l.) is a small freshwater, eutrophic, lake located in the town of Diss, East Anglia, England (Fig. 1a). The lake has a maximum water depth of 6 m with a lake surface area of 0.034 km^2 and a catchment of 1.5 km^2 (Fig. 1b, c). There are no surface inflows or outflows. The mere is situated in the River Waveney Valley, an area formed of chalky till. Drainage is poor around the mere which has resulted in waterlogged calcareous soils. The lake is located 7 km east of a major drainage divide (source of both the River Waveney and Little Ouse), but the topography does not reveal the current lake to be part of any

surface water system and it is unclear how much modem surface drainage enters the lake (Bailey, 2005). Local groundwater data from the Waveney Catchment is presented in Supplementary Table 1.

East Anglia is characterised by a relative continental climate (Mayes, 2000). The average climatology records maximum monthly air temperatures in July (17.4 °C) and minimum temperatures in January of 4.4 °C. Total annual precipitation for this region is 626.9 mm with the wettest and driest months being October (64.6 mm) and March (39.3 mm), respectively (Fig. 1d).

The Diss Mere varve models

The Diss Mere varves are shown in Figure 2. One varve typically consists of a pale lamina made of endogenic calcite crystals, and a dark lamina composed of, primarily, chrysophyceae cysts, planktonic centric diatoms, filaments of organic matter and micrite (Peglar et al. 1984). Coarse grains of endogenic calcite also occur in these laminae (Fig. 2b). The calcite layer is made of coarser grains at the bottom and crystal size decreases upwards through the lamina (Bailey, 2005) (Fig. 2b).

Diatom, pollen and chrysophyceae cyst content were described in detail for fourteen individual pale and dark laminae at 10.85 m of sediment depth (ca. 6 ka BP) to identify the phenology of biological cycles and help identify the seasonal succession of layers within a varve (Peglar et al., 1984). The diatom palaeo-community in these sediments is mainly represented (63-99%) by *Lindavia comta* (Kützing) Nakov et al., (2015). Diatoms occur in both the pale and dark layers, but with the greatest concentration in the dark-organic layer, alongside the highest abundance of chrysophyceae cysts. This suggests the formation of the dark lamina begins in late summer and autumn, when the cysts are commonly produced (Tippett, 1964).

The pollen composition of the pale layers is characterised by *Tilia* and Gramineae, whilst *Corylus, Alnus, Ulmus* and *Taxus* pollen is found in the dark layer reflecting a pattern of the phenological season distinguishing between plants flowering from May to July and in early spring, respectively (Peglar et al., 1984). The combination of pollen and chrysophyceae cyst observations reveal that the pale calcite layer might represent lake deposition in late spring and summer (May-July approx.), while the dark organic layer indicates accumulation from late summer to late spring (August-April approx.) (Peglar et al. 1984).

A microscopic sedimentological study of the varve structure through the entire varved sequence reveals, however, changing varve composition (Fig. 2a) possibly reflecting interannual variability of limnological processes inducing calcite precipitation and biological productivity. Three varve types have been recorded in Martin-Puertas et al. (2021). Varve type 1 is the light/dark couplet described above; varve type 2 includes a diatom layer prior to the light calcite layer; and varve type 3 is a couplet of diatom and organic dark layers with no (or very thin) calcite layers (Fig. 2c).

Methods

Lake monitoring survey

This lake monitoring survey at Diss Mere has been carried out monthly between June 2018 and November 2021 to study the modern sediments using sediment traps and physicochemical (temperature, pH, alkalinity, conductivity, dissolved oxygen, major ions) profiles of the lake's water column.

Physical and chemical properties

The water column physicochemical characteristics were obtained using a Multi 3320 WTW meter equipped with a Tetracon® 325 probe for temperature, conductivity, dissolved oxygen (DO), and pH. Measurements were recorded at 1 m intervals from the lake surface to lake bottom. At each interval, water samples were collected using a Niskin bottle for further chemical analyses: alkalinity was measured in situ with a HACH digital titrator model AL-DT; major cations (Ca^{2+}, Mg^{2+}, Na^{+}, K^{+}, NH_4^{+}) and anions (NO_3^{-}, PO_4^{3-} Cl^{-}, SO_4^{2-}) were analysed by ion chromatography with a Metrohm 930 Compact IC Flex equipped with a 919 IC Autosampler after 0.2 µm filtration. Analysis for cations began in May 2019, and anions in September 2019. Total reactive phosphates and acid-hydrolysable phosphorous (TP) were analysed by colorimetry with a Skalar Segmented Flow Analyser following digestion by Microwave assisted method in potassium persulfate/sulphuric acid mixture (Eaton et al, 1995).

Two nKe thermistors were attached to the sediment traps at 1 m and 5.5 m (Fig. 1b). Temperature was recorded every 10 minutes from June 2018 to June 2021 at 1m, and between June 2018 and June 2020 at 6m.

Sediment analyses

Two sets of PVC sediment traps were placed in the lake with the trap openings at 1m (epilimnion) and 5 m (hypolimnion) of lake water depth to analyse the sediment flux and composition (Fig. 1e). Each set of traps contained two PVC tubes each with an active area of 6.3 cm and length of 1 m, and a tap near the base to drain some of the lake water and suspended material collected during trap retrieval. The traps were emptied at each monitoring campaign and content, including the remaining lake water, and settled material in the trap, was stored in plastic bottles at 4 °C prior to analysis for sediment and diatom composition. In the lab, the content from each trap was homogenised and divided for diatom and chemical analysis.

An aliquot of the homogenised sample was filtered at 0.2 μm, dried, and scaled up to the whole volume of the water in the trap and the total mass flux (TMF: g m^{-2} d^{-1}) was calculated following equation 1.

(Equation 1)

$$TMF\ (g\ m^{-2}\ d^{-1}) = \frac{\text{Dry net weight of sediments (g)}}{\text{Active area } (m^2)\ \times\ Time\ between\ trap\ collection\ (d)}$$

Samples for chemical analysis, including organic and inorganic carbon, were filtered with a 0.2 μm GC fibreglass filter using a vacuum pump and then dried. Smear slides and sediment samples for scanning electron microscope (SEM) analysis were carried out to characterise the main components of the sediments. Sediment samples were mounted on aluminium stubs and carbon coated to 6 μm and observed under a Hitachi SU9000 SEM with backscatter and secondary electron modes. Organic and inorganic carbon were quantified using a Thermo Electron Corporation Flash EA 112 Series nitrogen and carbon soil analyser with carbon, hydrogen, nitrogen and sulphur (CHNS) configuration. Amino acid cystine (29.5 %C) was used as a quality control throughout the analysis, returning an overall SD of 1.94 (%C) and a bias of 0.35 (%C). For inorganic carbon, the sediment samples were previously treated with 10% hydrochloric acid overnight to remove the carbonates, they were then rinsed and dried. As carbonates were removed, the measured C can be considered total organic carbon (TOC).

The calcite saturation index (SI) is used here as an indication of favourable conditions for calcite to precipitate in the lake water. SI ≥ 0 indicates supersaturation and thus favourable conditions for precipitation (Roeser et al. 2021).

The SI was calculated using Equation 3 (Langmuir, 1971).

(Equation 2)

223 $$SI_{calcite} = \log \frac{[Ca^{2+}] \times [CO_3^{2-}]}{K_c}$$

224

225 Where [] is the activity of the free ion and K_c is the solubility constant of the calcite at a given
226 temperature. The activity of the free ions was calculated by the products of the specific activity
227 coefficients and concentrations. The activity coefficients were obtained using the conductivity
228 measurements. The carbonate concentration was calculated using the alkalinity, pH and
229 temperature.

230 To assess the role that phosphates have on the precipitation of calcite in Diss Mere, we
231 sequentially extracted both apatite (phosphorous bound to calcite) and non-apatite (inorganic)
232 phosphorous from the sediments. We followed the Williams method with adaptations
233 recommended by Ruban et al., (1998). Five months were selected from different seasons
234 (October 2019, February, March, July, and October 2020) from both sediment traps to reveal
235 seasonal changes through one year.

236 Diatom analysis

237

238 All water samples from the sediment traps were studied for diatom composition. To
239 concentrate the diatoms, 50 cm^3 of lake water from the traps were first spun down, allowing
240 ~0.1 g sample to be extracted for analysis. Preparation followed an adapted version of the
241 digestion procedure of Battarbee et al., (2001), where organics were removed using H_2O_2,
242 carbonates removed using several drops of 50% HCl, and samples were rinsed at least 4 times,
243 to neutralise the medium. Ammonia (NH_3) was added in the final stages to prevent diatoms
244 clumping. Concentrations were determined with the addition of divinylbenzene (DVB)
245 microspheres, added following the final rinse (Equation 3). Fluxes were calculated to account
246 for varying numbers of days between samples being collected. Samples were pipetted onto
247 cover slips and left to dry before being mounted in Naphrax™ mounting resin (refraction index

1.73). Samples were examined at 1000 x magnification using a Leica DMBL, and where possible, a minimum of 300 diatom valves were counted per sample. Identifications were made following Krammer and Lange-Bertalot (1986; 1991)**,** Lange-Bertalot, (2001), and Krammer (2002), Fritz (1989) and online resources (http://craticula.ncl.ac.uk and https://diatoms.org).

To determine the concentration the following equation was used:

(Equation 3)

$$Diatom\ Concentration = \frac{(\text{Total Microspheres Added} \times \text{Total Diatoms Counted})}{\text{Total Microspheres Counted}}$$

Diatom dissolution has been quantified across the samples to produce an *F*_index to estimate the diatom preservation state and the influence of dissolution on the sample and assemblage (Supplementary Information).

Meteorological data

Meteorological data was obtained from the Tibenham Airfield meteorological station (13 km from Diss Mere). The data collected includes daily mean values for air temperature (°C), wind speed (m s^{-1}), and total precipitation (mm).

Results

Physico-chemical properties of the water column: the annual lake cycle

Diss Mere is characterised by summer thermal stratification and winter mixing reflecting a monomictic mixing pattern (Fig. 3a). Surface temperatures ranged between 3–25 °C through the monitored years with the coldest water (3–5 °C) in February and warmest water (>21 °C) in summer (June-August). Water column mixing began to slow in March, and complete stratification was reached by April (Fig. 3a). Mean surface and bottom waters were 22.7 °C

and 12.0 °C, respectively during July, where the maximum thermal gradient was reached, sustaining a thermocline between 2–4 m (Figure 3a). By late August, the thermocline deepened, and intermittent periods of mixing continued until October, when mixing persisted until the following spring.

The annual lake turnover helps to regulate the chemical composition of the lake, where the chemical homogenisation of the water column coincides with the onset of lake mixing (Fig. 3). However, the stratification of different chemical parameters (the differences between the chemical composition of the epi- and hypolimnion) occurred at the same time as the intermittent and weak temperature gradients in March, occurring one month prior to complete thermal stratification (Fig. 3). During lake stratification, surface waters had the highest concentrations of DO ranging between 11 – 15 mg L^{-1} in the epilimnion and 0.9 – 2.8 mg L^{-1} in the hypolimnion (Fig. 3b). The oxycline (the depth at which DO = 2 mg L^{-1}) was located between 4 – 5 m during stratification. The duration of the hypolimnetic hypoxia showed high interannual variability, within one month in 2019 and 2020 to five months in 2021 (Fig. 3b).

Anoxic conditions in the hypolimnion (<1 mg L^{-1}, Nürnberg, 1995) were only observed once in June 2018 (0.6 mg L^{-1}). In the epilimnion, discrete peaks of DO occurred in April and September (Fig. 3b). The beginning of mixing in October marked the full oxygenation of the water column, with an increase from October (4 mg L^{-1}) to March (13 mg L^{-1}).

The equilibrium pH for carbonate lake systems at 8.3 (Ito, 2002) was usually reached in February in Diss Mere, coinciding with the end of the mixing season (Fig. 3c). During stratification, pH remained high in the epilimnion (pH values ~9) coinciding with peaks in DO and drops in alkalinity (Fig. 4a). In the hypolimnion, pH remained stable at 7, and increased slightly towards the end of summer. At lake overturn, pH increased with maxima in September/October (9.3) and March (8.9) (Fig. 3c). The alkalinity ranged 140 – 194 mg L^{-1} as $CaCO_3$ in the epilimnion and 153 – 233 mg L^{-1} as $CaCO_3$ in the hypolimnion (Fig. 4a).

298 Conductivity remained mostly consistent through the water column, and across most of the
299 year (Fig. 3d) with values ranging between ~ 600 – 720 μS cm^{-1}. Values increased to > 800 μS
300 cm^{-1} below 5 m of depth during the stratified season coinciding with the hypoxic layer.
301 The most abundant cation was Ca^{2+} (Supplementary Table 2). The vertical distribution
302 of this ion was not as heterogenous as other dissolved substances in the water column (Fig 3
303 and 4); however, some variability was observed across the year. Maximum concentrations were
304 reached in February and March (> 65 mg L^{-1}) which then decreased until the lowest
305 concentration (55 – 43 mg L^{-1}) between June to August (Fig. 4b; Supplementary Table 2). The
306 concentration of Ca^{2+} increased gradually during the mixed season.
307 Nutrient concentrations of both dissolved phosphate (PO_4^{3-}) and total phosphate
308 decreased in February and March with the complete absence of PO_4^{3-} at certain depths in March
309 2021 (Fig. 4c-d). The highest NO_{3-} concentrations were in February (3.9 mg L^{-1}) but were
310 rapidly depleted by March (0.7 mg L^{-1}). During stratification NO_{3-} remained depleted and was
311 replenished following lake overturn in October with an average of 1.4 mg L^{-1} (Supplementary
312 Table 2).
313
314 Deposition of modern sediment components
315
316 Smear slides and SEM images revealed that the main component of the sediments in the traps
317 was calcite and organic matter remains (Fig. 5, left panel). Calcite grain size varied through the
318 year with larger grains (5 – 15 μm) collected in spring and summer compared to those in
319 autumn (< 5 μm) (Fig. 5c, e). During the autumn-winter samples, *Pediastrum* (green algae)
320 was the dominant component of the sediments forming a matrix together with fine micrite
321 calcite crystals (Fig. 5g, h). Some rhombohedral calcite grains (< 5 μm) were present and were
322 typically attached to diatom valves in the autumn and winter samples (Fig. 5h, i).

Total Mass Flux (TMF)

Figure 6 displays the changes in both the timing and composition of sediment collected in the traps, revealing evidence of seasonal and interannual variability. TMF in the epilimnion and hypolimnion followed the same general pattern, however the amount of material collected at the hypolimnion was greater (Fig 6a). Increases in TMF occurred in Spring (March–May) when the lake began to stratify, a higher flux was recorded in the hypolimnion recording a maximum seasonal flux of 8.1 g m^{-2} d^{-1} in April 2021. A gradual decline in TMF occurred during the summer until August. The largest flux of sediment was recorded at the point of lake mixing in September or October (Fig. 6a). The traps in October 2021 collected the highest flux of the monitoring period (22.2 g m^{-2} d^{-1}).

Organic Matter (OM) flux

Clear seasonal differences exist in the amount of OM collected within the traps (Fig. 6b). During the stratified period OM flux remained stable and low with mean values of 0.8 g m^{-2} d^{-1} in the epilimnion, and 1.3 g m^{-2} d^{-1} in the hypolimnion. It reached its annual maximum in September/October following lake overturn, with the highest flux recorded in October 2021 (7.7 g m^{-2} d^{-1}). Whilst not as substantial as in autumn, there was a secondary flux in spring reaching maximum values of 2.0 g m^{-2} d^{-1} and 2.9 g m^{-2} d^{-1} in the epi- and hypolimnion, respectively. This seasonal pattern of changes in OM flux was consistent through the monitored period except for 2018 when OM remained low consistently through the year (Fig. 6b).

Calcite flux

Similar to OM, calcite flux also demonstrated a seasonal component to its deposition. An initial primary flux was recorded with mean values of 2.4 g m^{-2} d^{-1} and 3.3 g m^{-2} d^{-1} in the

epi- and hypolimnion, respectively in spring (March–May) (Fig. 6c). Through the summer months (June-August), calcite flux increased to a maximum of 6.6 g m^{-2} d^{-1} in July 2020. Calcite flux decreased towards the end of summer and a further peak occurred following the demise of thermal stratification at beginning of lake mixing in both the epilimnion (3.4 g m^{-2} d^{-1}) and hypolimnion (4.7 g m^{-2} d^{-1}). Calcite flux was typically greater in the hypolimnion traps through most of the year, except in summer when most of the calcite was collected in the epilimnion (Fig. 6c).

In all the monitored years, except 2018, peaks of calcite precipitation occurred both during the stratified period, and again following lake turnover in autumn. In 2018, the main calcite flux occurred only during lake stratification with no clear increase in autumn (Fig. 6c). The year 2019 was an anomaly with exceptionally low calcite in the traps – the lowest calcite flux of the monitored period was 0.2 g m^{-2} d^{-1} in February 2019, and very low calcite precipitation in summer (0.7 g m^{-2} d^{-1}). Most of the calcite flux collected during this year was in October (Fig. 6c). The amount of apatite phosphate found in the sediments was greatest in the October samples, with a maximum of 17.8 g Kg^{-1} in the hypolimnion (Supplementary Table 3). July recorded the lowest amount of apatite phosphate with 2.2 g Kg^{-1} and 3.2 g Kg^{-1} in the epi- and hypolimnion, respectively.

SI in the epilimnion remained mostly above zero (-0.6 to 1.5), except for September 2020 (-0.6), and November 2021 (-0.1). Peaks of epilimnion SI occurred in early spring and autumn (Fig. 6c). Hypolimnion SI values ranged between –0.6 to 0.9.

Diatoms

Diatom blooms occurred in early spring (February–March) and in autumn (September–November), the latter following lake overturn. Concentrations were generally lower during the summer, especially in July and August 2019 (Fig. 6d). The Diss Mere assemblage consists of

128 diatom species (Supplementary Table 4 and 5). The dominant species is *Cyclostephanos dubius* (Hustedt) Round, 1988, a generally small, but morphologically variable, planktonic, centric species (Bradshaw and Anderson, 2003) (Fig. 5i). The highest concentrations of diatoms were recorded in the epilimnion in spring/early summer, and in autumn for the hypolimnion (Fig. 6d). In general, both the spring and autumn blooms were dominated by *C. dubius*, but smaller fluctuations of other species characterised the seasonal blooms. Short-lived peaks in *Stephanodiscus hantzschii* Grunow, occurred in the spring only, while small concentrations of benthic taxa were observed in the autumn, including *Amphora* species, Naviculoid species and *Achnanathes* species. Diatom preservation varied throughout the samples (Supplementary Information Fig. 1).

Meteorological Data

Air temperatures between 2018 to 2021 followed a seasonal pattern (Fig. 7b). Maximum average monthly temperatures peaked in July/August (19.0 °C), and minimum monthly average temperatures in January (4.3 °C). January 2019 and February 2021 were the coldest months of the monitoring period with the coldest day of the monitoring period recording a daily average of -2.9 °C in February 2021, despite negative temperatures, ice cover on the lake did not occur. Wind speeds during the summer months (June-August) were the lowest, with a mean of 3.7 m s^{-1} which then increased in autumn (September–November) to 4.1 m s^{-1}. February had the highest overall mean at 5.1 m s^{-1} (Fig. 7c). Monthly precipitation during the monitored period showed no clear seasonal pattern, but in general there was an increase in the autumn and winter months, compared to the spring and summer (Fig. 7d).

Discussion

Meteorological impact on the dominant limnological processes

The monomictic mixing regime in Diss Mere is strongly driven by air temperature and windy conditions. Water temperatures closely follow the annual variability of air temperature with thermal stratification driven by spring temperature increases and the decline of temperatures, alongside a general increase in winds in autumn result in lake overturn. The large volume of Diss Mere in relation to its relatively small watershed suggests that the lake ecosystem dynamics might be mainly controlled by the annual water cycle rather than catchment processes such as terrestrial runoff. In addition, the high conductivity of the lake water (~720 μS cm^{-1}) accounts for approximately 90% that of ground water from this locality (~810 μS cm^{-1}, Supplementary Table 2), suggesting groundwater is the main inflow into the lake and only a small proportion of lake water comes from either direct precipitation, or through runoff (Bailey, 2005).

Lake productivity

Peaks in productivity occur twice in the year at Diss Mere, with the first in spring. This is characterised by a diatom bloom and peak in organic matter flux following maximum windspeeds in February and a general increase in surface water temperatures. Despite *C. dubius* remaining the dominant species of the bloom, the springtime diatom assemblage includes higher concentrations of *S. hantzschii*, likely because water temperatures are cooler (<12 °C) throughout February and March (Jung et al., 2009). The presence of *S. hantzschii* and *C. dubius* would explain the depletion of dissolved phosphates in early spring (February and March), followed by the depletion of nitrates in April, a nutrient commonly associated with *C. dubius* (Bradshaw and Anderson, 2003).

During the summer, concentrations of nutrients in the epilimnion are low, with an accumulation of phosphates in the hypolimnion at the sediment-water interface, and very low concentrations of NO_3^- throughout the water column. The breakdown of thermal stratification in September permits diatom-limiting nutrients to reach the photic zone (Bradshaw and Anderson, 2003; Roeser et al., 2021), and temperatures are still warm enough to allow the occurrence of a diatom bloom, specifically *C. dubius*. The second peak in productivity occurs in autumn, coinciding with the onset of the lake turnover. This peak in productivity is larger than the spring peak, evidenced by the highest OM flux, diatom concentration and presence of *Pediastrium* from September to November.

Both the spring and autumn diatom blooms are influenced by wind-induced lake mixing, recirculating nutrients to the photic zone and allowing smaller planktonic species, such as *C. dubius*, to outcompete others due to its preference for eutrophic conditions and its ability to tolerate low light levels through greater turbidity (Bradshaw and Anderson, 2003). This suggests a lake response encouraged by windy activity and a potential signal in the sediment represented by the deposition of a diatom layer.

Calcite precipitation

Calcite is deposited throughout the year at Diss Mere, however, similarly to the diatom concentrations, calcite precipitation also reveals a seasonal pattern. The annual variability of dissolved Ca^{2+} and the decrease in concentration in the epilimnion between May and October suggests calcite is precipitating during these months. Primary calcite peaks occur during the stratified seasons from late spring to late summer in the epilimnion followed by secondary peaks in autumn, mainly recorded in the hypolimnion. The permanent calcite precipitation in the lake during the whole year is likely a result of calcium oversaturation throughout the water

column. Given the composition of the local bedrock and groundwater analyses from the Waveney Catchment (Supplementary Table 2), the water of Diss Mere is likely to be a dilute solution of calcium bicarbonate. This is complimented by almost consistent positive values of SI in the epilimnion, reporting oversaturation, hence favourable conditions for persistent precipitation.

Seasonal calcite peaks, however, could be accentuated by either pH increases, displacing the carbonate equilibrium from organism activity, favourable temperatures, or both (Kelts and Hsü, 1978; Dittrich and Obst, 2004). In Diss Mere, the increases in pH, driven by diatom blooms in early spring, and the general increase in air temperatures, in turn warming the epilimnion, triggers the oversaturation of $CaCO_3$ and facilitates calcite precipitation (Stabel, 1986; Trapote et al., 2019; Żarczyński et al., 2022). It is notable that in years where spring diatom concentrations are higher (April 2019; May 2021), early spring calcite precipitation events occur.

The calcite collected during spring presents large well-developed calcite grains (5-15µm) (Fig. 5c). High concentrations of dissolved phosphates have been shown to limit calcite precipitation leading to the supersaturation of lake water (Kunz and Stumm, 1984; Lotter et al., 1997). Once consumed, the rapid precipitation of large calcite grains can occur (Lotter et al., 1997). This is likely the cause of the larger spring calcite crystals at Diss Mere during these months as the concentration of dissolved PO_4^{3-} from Autumn through the winter remain high (0.7 mg L^{-1}) and are then rapidly depleted in February or March (0.05 mg L^{-1}) coinciding with the first algal bloom of the year.

The summer months are when calcite precipitation is more pronounced at Diss Mere, reflected by the dip in epilimnion Ca^{2+} and alkalinity, and the higher amount of calcite collected in the traps, coinciding with the warmest air temperatures. Saturation index in the epilimnion

472 is also highest, likely from warmer waters. Calcite crystals here are still well-developed from
473 the slow precipitation maintained by temperature (Fig. 5).

474 The second calcite peak is in autumn and is collected mostly in the hypolimnion and
475 the calcite in the trap is largely dominated by micrite (Fig. 5). However, the autumn is the most
476 productive period of the year, and both the saturation index, and relatively low epilimnion
477 concentrations of Ca^{2+}, suggest that endogenic calcite is still precipitating during this period.
478 The endogenic calcite crystals collected during these months are smaller (< 5μm), likely
479 resulting from the increase in dissolved PO_4^{3-} compared to the spring and summer seasons. The
480 relationship between changing crystals size and phosphate is complimented by the greatest
481 amount of apatite phosphate found in the October sediment samples (Supplementary Table 3).
482 This suggests more phosphate is absorbed into the active growth sites during precipitation,
483 limiting grain size growth (House, 1980; Plant and House, 2002, Lotter et al., 1997). This is
484 not the case however, for the calcite precipitation in the summer when there is much lower
485 apatite phosphate present in the sediments (Supplementary Table 3).

486 *Resuspension*

487

488 Despite clear evidence showing that the sediment trapped during a single year represents the
489 limnological processes occurring in the water column, some evidence suggests the sediments
490 collected from October to February could also include resuspended material from both the
491 littoral zone and lake bottom (Roeser et al., 2021). This is demonstrated by greater amount of
492 calcite in the hypolimnion trap, as well as minerogenic particles and plant remains deposited
493 during the lake mixing season (Fig. 5g). Whilst this could also be the accumulation of calcite
494 from other depths of the water column below the epilimnion trap opening, the presence of
495 several benthic diatom species in autumn including *Amphora* species, Naviculoids and
496 *Achnanathes* species supports this interpretation (Supplementary Table 5). Layers of

resuspended material in organic-calcite varves have been described in other European lakes and associated with site-specific lake morphology promoting the erosion of littoral parts of lakes from surface currents and waves (Roeser et al., 2021). The seasonal resuspension during lake turnover might be also accompanied by an autumn diatom bloom as it has been observed in Lake Czechowskie, which is driven by the redistribution of water column nutrients into the photic zone (Roeser et al., 2021). In Diss Mere the shallow waters (max. depth 6 m) and the morphology of the basin make the lake bottom vulnerable to wind-induced erosion, explaining both the deposition of resuspended material during the mixing season and the main diatom bloom in autumn.

Validation of the varve conceptual model

The main limnological processes identified in a single year in the modern Diss Mere system leaves a trace in the traps consisting of three different depositional phases: i) an early spring diatom bloom; ii) late spring and summer calcite precipitation characterised by calcite grains with an average size of 10 μm; and iii) an autumn diatom bloom, micritic calcite and resuspended material. This seasonal depositional sequence resembles the conceptual model of the varved record at Diss Mere, thereby suggesting that the modern limnology could be applied to the sediment record. Unlike the dominant microfacies recorded in the varved sequence where varve type 1 reflects ~90% of the varves, the seasonality observed in this study is likened to varve type 2 (Fig. 2). Varve type 1 does not present a spring diatom bloom as an independent layer; however, this might be mixed with the calcite layer thus prevents its identification on the thin sections. The calcite layer in the varves show coarse grains at the base and fine calcite grains at the top, representing the decreasing grain size observed from May to October in the sediment traps. The transition between the calcite layer and dark organic layer is diffuse as calcite grains still occur in the dark layer but intermixed with a wide range of diatoms species

(including benthic species) and terrestrial organic matter remains (Fritz et al., 1989). This suggests resuspension is one of the dominant deposition processes during this season (Roeser et al., 2021).

Less than the 8% of the Holocene varves in Diss Mere correspond to varve type 3, where the calcite layer is extremely thin or absent. During the monitoring period, we have observed one year (2019) in which the spring and summer calcite is very low and thus may correspond to this varve type. Diatom concentration is high in spring 2019 and Ca^{2+} ions decrease in summer 2019, which suggest that calcite grains might have precipitated, but not collected in the traps. According to the results shown in this study, we find no clear link with the meteorological data, limnology, and diatom productivity to explain the lower precipitation during this summer. We therefore speculate that the occurrence of this varve type may be specific to certain lake conditions not recorded during this monitoring period.

A main issue in studying calcite varves is the deposition of multiple calcite layers (Trapote et al., 2018; Roeser et al., 2021; Żarczyński et al., 2022). Sediment trapping in Diss Mere reveals two calcite pulses, a summer event sustained by temperature, and an autumn event driven by biological productivity. Because these two calcite pulses precipitate in sequential seasons it is likely that the calcite would be deposited as a single layer, leaving a trace characterised by the gradual decrease in the grain size. From the palaeolimnological point of view, this means that multiple calcite precipitation events in a year are recorded as a single layer in the sediments and therefore unlikely to have chronological implications on varve counting. This is validated by the comparison of the varve counts with radiocarbon dates and selected tephra ages, all integrated into a Bayesian age model for the Diss Mere record (Martin-Puertas et al., 2021), but the environmental interpretation of calcite deposition in the sediments might be complex.

Although longer timeseries of monitoring data together with a permanent sediment trap are needed to establish statistically significant relationships between meteorology, limnology and lake sediments, our study suggests that most of the calcite deposited as a layer correspond to the summer and relates to annual maximum temperature; and the autumn precipitation might mark the diffuse transition between the light and the dark layers in the varves. Thus, either the thickness of the calcite layer, the contribution of the calcite layer to the total varve thickness, the Ca^{2+} in the sediments, or all, might potentially be sensitive to summer temperature variability during the Holocene.

Limiting factors for varve preservation

Varves stopped preserving around 2,100 years ago in Diss Mere, with some intermittent periods of preserved laminations over the last two thousand years. Despite a strong seasonality in the sediment deposition, which is the case in the modern Diss Mere system, varve preservation depends on hypoxia preventing bioturbation and the absence of erosive processes at the lake bottom (Ojala et al., 2000; Zolitschka et al. 2015). Much of the global varves preserved today have been preserving for the last few centuries only, which is the result of cultural eutrophication increasing lake productivity, degradation of the organic matter and, consequently resulting in hypoxic hypolimnions (Jenny et al. 2013; Dräger et al., 2016; Haas et al., 2019; Poraj-Górska et al., 2021; Salminen et al., 2021). However, natural varve preservation mainly depends on the catchment and lake morphology, with a low lake surface/depth ratio reducing wind-induced bottom oxygenation and sediment resuspension (Ojala et al., 2000). Recent studies on varved sediment formation and preservation show evidence that permanent hypolimnetic anoxia and meromictic conditions are not essential to preserve varved sediments. Instead, monomictic/dimictic lakes with short periods of available oxygen at the bottom are also able to preserve varves (Bonk et al., 2015; Roeser et al., 2021;

571 Żarczyński et al., 2022) of which a seasonal layer of resuspended material can be deposited
572 and preserved (Roeser et al., 2021). The fact that the seasonal-defined sediments at Diss Mere
573 are not preserved as varves following cultural eutrophication, and varves stopped preserving
574 two thousand years ago suggests that varve preservation conditions during the Holocene were
575 maintained by an optimal lake surface/depth ratio. The evidence of resuspended material in the
576 varves indicates that the water column might not have been deep enough to sustain meromictic
577 conditions, but periods of lake mixing and ventilation of the lake bottom were short preventing
578 bioturbation thus allowing varve preservation. The end of the varve preservation occurred
579 gradually when varves fade out over a few years (Martin-Puertas et al., 2021) coinciding with
580 forest clearance and farming of the catchment suggesting an intensification of human activities
581 from ca. 2.1 ka BP (Peglar et al., 1993). We suggest that the contribution of these two factors
582 played a role in varve preservation at Diss Mere. Natural infilling of the lake alters the lake
583 surface/depth ratio and may have been intensified by the increase in deforestation and soil use
584 increasing the detrital input, supported by the rapid increase in sedimentation rate (Martin-
585 Puertas et al., 2021). Both, a lake with an optimum surface/depth ratio, and a more open forest
586 would favour longer wind-induced water mixing with available oxygen in the hypolimnion.
587 The monitoring survey reveals that the current lake bottom is oxygenated (>2 mg L^{-1}) for most
588 of the year, explaining the lack of varve preservation even when lake seasonality characterises
589 sediment deposition. The intermittent preservation of laminations in the last two millennia
590 suggest that relative changes in lake level and/or changing intensity of human activities on the
591 catchment could have an impact on preservation conditions.

592 **Conclusions**

593 This study applies a 3.5-year lake monitoring survey on Diss Mere, England to disentangle the
594 main drivers of sediment deposition in the Holocene varved sediments through a modern
595 analogue approach. We found that Diss Mere is a monomictic lake currently forming

seasonally defined sediments that consist of i) a spring diatom bloom, ii) calcite precipitation from late spring through summer, and iii) an autumnal diatom bloom with calcite grains bonded to organic matter and resuspended material from the littoral area. This annual pattern is similar to that recorded in the varve record and we conclude that a modern analogue could be applied to understand the seasonal environmental and climate signals recorded in the Holocene varves. The current lake seasonality is driven by air temperature and windiness. Lake productivity is enhanced during lake mixing from autumn to early spring by wind bringing additional nutrients into the photic zone, and most of the calcite precipitates over the summer through favourable temperatures. Although a long-term monitoring survey is needed to establish stronger relationship between meteorology and interannual variability of seasonal sediments (e.g. mass fluxes), this study suggests that the Diss Mere varves might have high potential for palaeoclimate investigations. Despite the seasonally defined sediments deposited today, we find that they are unable to be preserved as varves due to the lack of a stable hypoxic period maintained through the year, likely resulting from the shallow water depth of the lake. One limitation of the modern analogue approach is that it does not capture the influence of the ice cover on varve formation processes, which could induce variability in the lake seasonality during colder climates. As a final message, we highlight the importance of bridging the gap between limno- and palaeolimnology through sediment trapping techniques to develop robust and reliable reconstructions. We emphasise this especially for lakes which experience strong seasonality today and therefore may be potential sites for varve exploration.

Acknowledgements

This study was funded by the Royal Society (ref: DH150185; R10972). L. Boyall is funded by Royal Holloway University of London through a PhD studentship. A. Hernández is funded by

the Spanish Ministry of Science and Innovation through the Ramón y Cajal Scheme [RYC2020-029253-I]. The authors thank the Diss Council, Sarah Richard, Robert Ludkin and his team for being generous and supportive, and Pete Langdon for giving us access to SEM facilities at the University of Southampton and Amy Gough for SEM support at Royal Holloway University of London. Thanks to the colleagues and students who made monthly monitoring possible. Special thanks to Simon Blockley, Amy Walsh, Joshua Pike and Marta Perez for many surveys, and Helen Bennion, George Biddulph, Alice Carter-Champion, Rachel Devine, Stefan Engels, Chris Francis, Daniella Giannito, Natalie Hamilton, Tim Holt-Wilson, Christine Lane, John Lowe, Adrian Palmer, Rhys Timms, Madeleine Timmins, Rik Tjallingii. We dedicate this paper to the curious and fascinating Diss folk who shared many stories about the mere and made us aware of the social impact of our work. We would also like to thank Dr. Margarita and the two anonymous reviewers for providing valuable comments on the manuscript.

Funding Declaration

This study was funded by the Royal Society (ref: DH150185; R10972). L. Boyall is funded by Royal Holloway University of London through a PhD studentship. A. Hernández is funded by the Spanish Ministry of Science and Innovation through the Ramón y Cajal Scheme [RYC2020-029253-I].

Conflicts of Interest

Authors declare no conflict of interest

Author Contribution

L.B and C.M.P. wrote the main manuscript text. C.M.P. designed the study, L.B and J.V. ran the chemical analyses. A.H. and C.M.P. designed and installed the sediment traps. P.H. extracted and identified the diatoms. All authors were involved in analysing results. All authors contributed to both the writing of the manuscript and to discussions about results. All authors reviewed the manuscript before submission.

References

Apolinarska K, Pleskot K, Pełechata A, et al (2020). The recent deposition of laminated sediments in highly eutrophic Lake Kierskie, western Poland: 1 year pilot study of limnological monitoring and sediment traps. J Palaeolimnol. 63: 283-304. https://doi.org/10.1007/s10933-020-00116-2

Battarbee R, Juggins S, Gasse, F, et al (2001). An Information System for Palaeoenvironmental Reconstruction. EDDI. 81. pp. 1–94.

Bonk A, Tylmann W, Amann B, et al (2015). Modern limnology and varve-formation processes in lake Żabińskie, northeastern Poland: Comprehensive process studies as a key to understand the sediment record. J Limnol, 74:358–370. https://doi.org/10.4081/JLIMNOL.2014.1117

Bradshaw EG, & Anderson NJ. (2003). Environmental factors that control the abundance of Cyclostephanos duhius (Bacillariophyceae) in Danish lakes, from seasonal to century scale. European Journal of Phycology. 38:265–276. https://doi.org/10.1080/0967026031000136349

671

672 Brauer A. (2004). Annually Laminated Lake Sediments and Their Palaeoclimatic Relevance.
673 In: The climate in Historical Times. 109–127. https://doi.org/10.1007/978-3-662-10313-5_7

674

675 Brauer A, Mangili C, Moscariello A, & Witt A. (2008). Palaeoclimatic implications from
676 micro-facies data of a 5900 varve time series from the Piànico interglacial sediment record,
677 southern Alps. Palaeogeogr, Palaeocl, Palaeoecol, 259:121–135.
678 https://doi.org/10.1016/J.PALAEO.2007.10.003

679

680 Cohen AS. (2003). Paleolimnology: The History and Evolution of lake systems-. 184–189.
681 Oxford University Press, New York.

682

683 Corella JP, Benito G, Rodriguez-Lloveras X, et al (2014). Annually-resolved lake record of
684 extreme hydro-meteorological events since AD 1347 in NE Iberian Peninsula. Quat Sci Rev.
685 93:77-90. https://doi.org/10.1016/j.quascirev.2014.03.020

686

687 Czymzik M, Dreibrodt S, Feeser I. et al. (2016). Mid-Holocene humid periods reconstructed
688 from calcite varves of the Lake Woserin sediment record (north-eastern Germany). 26(6), 935–
689 946. https://doi.org/10.1177/0959683615622549

690

691 Dittrich, M., & Obst, M. (2004). Are Picoplankton Responsible for Calcite Precipitation in
692 Lakes? AMBIO: Journal of the Human Environment. 33:559–564.
693 https://doi.org/10.1579/0044-7447-33.8.559

694

695 Dräger N, Theuerkauf M, Szeroczyńska K, et al (2016). Varve microfacies and varve
696 preservation record of climate change and human impact for the last 6000 years at Lake Tiefer
697 See (NE Germany). The Holocene 27:450–464. https://doi.org/10.1177/0959683616660173
698
699 Eaton AD, Clesceri LS, Greenberg AE (1991) 4500-P Phosphorous (eds). Standard methods
700 for the examination of water and wastewater. AM Public Health Assoc, Washington. 106-113.
701
702 Fritz SC. (1989). Lake development and limnological response to prehistoric and historic land-
703 use in Diss, Norfolk, UK. Journal of Ecology, 77:182–202. https://doi.org/10.2307/2260924
704
705 Haas M, Baumann F, Castella D, et al (2019). Roman-driven cultural eutrophication of Lake
706 Murten, Switzerland. Earth Planet Sci Lett. 505:110-117.
707 https://doi.org/10.1016/j.epsl.2018.10.027
708
709
710 Jenny, J-P., Arnaud, F., Dorioz, J-M., et al (2013) A spatiotemporal investigation of varved
711 sediments highlights the dynamics of hypolimnetic hypoxia in a large hard-water lake over the
712 last 150 years. Limnol and Oceanogr. 54:1395-1408.
713 https://doi.org/10.4319/lo.2013.58.4.1395
714
715 Jung SW, Kwon OY, Lee JH, et al (2009) Effects of water temperature and silicate on the
716 winter blooming diatom stephanodiscus hantzschii (bacillariophyceae) growing in eutrophic
717 conditions in the lower Han River, south Korea. Journal Freshw Ecol 24:219–226.
718 https://doi.org/10.1080/02705060.2009.9664286
719

Kelts K, & Hsü K. (1978) Freshwater carbonate sedimentation. In: Lerman A. (ed.), Lakes: Physics, Chemistry and Geology. Springer, New York, pp. 295-323.

Kienel U, Kirillin G, Brademann B, et al (2017). Effects of spring warming and mixing duration on diatom deposition in deep Tiefer See, NE Germany. J Paleolimnol 57:37–49 https://doi.org/10.1007/s10933-016-9925-z

Krammer K. (2002) Diatoms of Europe. Diatoms of the European inland waters and comparable habitats. Volume 3: Cymbella. Germany

Krammer K, & Lange-Bertalot H (1986) Bacillariophyceae. 1: Teil: Naviculaceae., Süßwasserf. Gustav Fischer Verlag, Stuttgart

Krammer K. Lange-Bertalot H. (1991) Bacillariophyceae. 4: Teil: Achnanthaceae., Süßwasserf. Gustav Fischer Verlag, Stuttgart

Kunz B, & Stumm W. (1984). Kinetik der Bildung und des Wachstums von Calciumcarbonat. Vom Wasser, 62:279-293

Langmuir D. (1971) The geochemistry of some carbonate ground waters in Central Pennsylvania. Geochim Cosmochim Acta. 35:1023-1045

Lotter AF., & Birks HJB. (1997). The separation of the influence of nutrients and climate on the varve time-series of Baldeggersee, Switzerland. Aquatic Sciences. 59:362–375. https://doi.org/10.1007/BF02522364

Lücke A, & Brauer A. (2004). Biogeochemical and micro-facial fingerprints of ecosystem response to rapid Late Glacial climatic changes in varved sediments of Meerfelder Maar (Germany). Palaeogeogr, Palaeoclimatol, Palaeoecol, 211:139–155. https://doi.org/10.1016/J.PALAEO.2004.05.006

Martin-Puertas C, Brauer A, Dulski P, & Brademann B. (2012). Testing climate–proxy stationarity throughout the Holocene: an example from the varved sediments of Lake Meerfelder Maar (Germany). Quat Sci Rev, 58:56–65. https://doi.org/10.1016/J.QUASCIREV.2012.10.023

Martin-Puertas C, Walsh AA, Blockley SPE, et al (2021). The first Holocene varve chronology for the UK: Based on the integration of varve counting, radiocarbon dating and tephrostratigraphy from Diss Mere (UK). Quat Geochronol , 61:101134. https://doi.org/10.1016/J.QUAGEO.2020.101134

Mayes, J. (2000). Changing regional climatic gradients in the United Kingdom. Geographical Journal, 166:125–138. https://doi.org/10.1111/J.1475-4959.2000.TB00013.X

Nakov T, Guillory W, Julius M, et al. (2015) Towards a phylogenetic classification of species belonging to the diatom genus Cyclotella (Bacillariophyceae): Transfer of species formerly placed in *Puncticulata*, *Handmannia*, *Pliocaenicus* and *Cyclotella* to the genus Lindavia. Phytotaxa. 215:249-284.

768 Nürnberg GK, (1995). The anoxic factor, a quantitative measure of anoxia and fish species
769 richness in Central Ontario Lakes. Trans Americ Fish Soci. 124:677–686.
770 https://doi.org/10.1577/1548-8659(1995)124<0677:TAFAQM>2.3.CO;2
771
772 Ojala AEK, Saarinen T & Salonen VP. (2000) Preconditions for the formation of annually
773 laminated lake sediments in southern and central Finland. Boreal Env Res. 5:243-255.
774
775 Ojala AEK, Kosonen E, Weckström J, Korkonen S, Korhola, A. (2013). Seasonal formation of
776 clastic-biogenic varves: the potential for palaeoenvironmental interpretations. GFF. 135:237–
777 247. https://doi.org/10.1080/11035897.2013.801925
778
779 Peglar SM. (1993) The development of the cultural landscape around Diss Mere, Norfolk, UK,
780 during the past 7000 years. Rev Palaeobot Palynol
781
782 Peglar SM, Fritz SC, Alapoeti T, Saarnisto M, & Birks HJB. (1984). Composition and
783 formation of laminated sediments in Diss Mere, Norfolk, England. Boreas. 13:13-28.
784 https://doi.org/10.1111/J.1502-3885.1984.TB00054.X
785
786 Poraj-Górska AI, Bonk A, Żarczyński M, et al (2021) Varved lake sediments as indicators of
787 recent cultural eutrophication and hypolimnetic hypoxia in lakes. Anthropocene. 36:100311.
788 https://doi.org/10.1016/j.ancene.2021.100311
789
790 Roeser P, Dräger N, Brykała D, et al (2021). Advances in understanding calcite varve
791 formation: new insights from a dual lake monitoring approach in the southern Baltic lowlands.
792 Boreas, 50:419–440. https://doi.org/10.1111/bor.12506

Ruban V, López-Sánchez FJ, PardoP, et al (1998) Selection and evaluation of sequential extraction procedures for the determination of phosphorous forms in lake sediment. J Environment Monit. 1:51-56.

Salminen S, Tammelin M, Jilbert T, Fukumoto Y & Saarni S. (2021) Human interactions were responsible for both initiation and termination of varve preservation in Lake Vesijärvi, southern Finland. J Palaeolimnol. 66: 2017-227. https://doi.org/10.1007/s10933-021-00200-1

Sear DA, Allen MS, Hassall J. et al (2020) Human settlement of East Polynesia earlier, incremental, and coincident with prolonged South Pacific drought. PNAS, 117(16), 8813–8819. https://doi.org/10.1073/PNAS.1920975117

Stabel H-H (1986) Calcite precipitation in Lake Constance: Chemical equilibrium, sedimentation, and nucleation by algae. Limnol Oceanogr, 31:1081–1094. https://doi.org/10.4319/LO.1986.31.5.1081

Sturm M. & Lotter AF. (1995). Lake sediments as environmental archives. EAWAG News 38(E). 6–9

Tippett R. (1964) An investigation into the nature of the layering of deep-water sediments in two eastern Ontario lakes. Canadian Journal of Botany. 42:1693–1709. https://doi.org/10.1139/B64-168

818 Trapote M C, Vegas-Vilarrúbia T, López P, et al (2018) Modern sedimentary analogues and
819 integrated monitoring to understand varve formation in the Mediterranean Lake Montcortès
820 (Central Pyrenees, Spain). Palaeogeo, Palaeoclimatol, Palaeoecol, 496:292–304.
821 https://doi.org/10.1016/j.palaeo.2018.01.046
822
823 Tylmann W, Szpakowska K, Ohlendorf C, Woszczyk M, & Zolitschka B. (2012) Conditions
824 for deposition of annually laminated sediments in small meromictic lakes: A case study of Lake
825 Suminko (Northern Poland). J Paleolimnol, 47:55–70. https://doi.org/10.1007/S10933-011-
826 9548-3/
827
828 Vegas-Vilarrúbia T, Rull V Trapote MdC, et al (2020) Modern Analogue Approach Applied
829 to High-Resolution Varved Sediments—A Synthesis for Lake Montcortès (Central
830 Pyrenees). Quaternary. 3(1). https://doi.org/10.3390/quat3010001
831
832 Walsh AA, Blockley SPE, Milner AM, Matthews IP, & Martin-Puertas C. (2021) Complexities
833 in European Holocene cryptotephra dispersal revealed in the annually laminated lake record of
834 Diss Mere, East Anglia. Quat Geochronol, 66:101213.
835 https://doi.org/10.1016/J.QUAGEO.2021.101213
836
837 Wilcox C. & Stanczszyn R. (1983) The sand and gravel resources of the country around Diss,
838 Norfolk. TM. 17.
839
840 Zander PD, Żarczyński M, Vogel H, et al (2021) A high-resolution record of Holocene primary
841 productivity and water-column mixing from the varved sediments of Lake Żabińskie, Poland.

Science of The Total Environment 755:143713. https://doi.org/10.1016/j.scitotenv.2020.143713

Żarczyński M, Zander PD, Grosjean M, & Tylmann W. (2022) Linking the formation of varves in a eutrophic temperate lake to meteorological conditions and water column dynamics. Science of The Total Environment, 842:156787. https://doi.org/10.1016/j.scitotenv.2022.156787

Zolitschka B, Francus P, Ojala AEK, & Schimmelmann A. (2015) Varves in lake sediments – a review. Quat Sci Rev 117, 1–41. https://doi.org/10.1016/J.QUASCIREV.2015.03.019

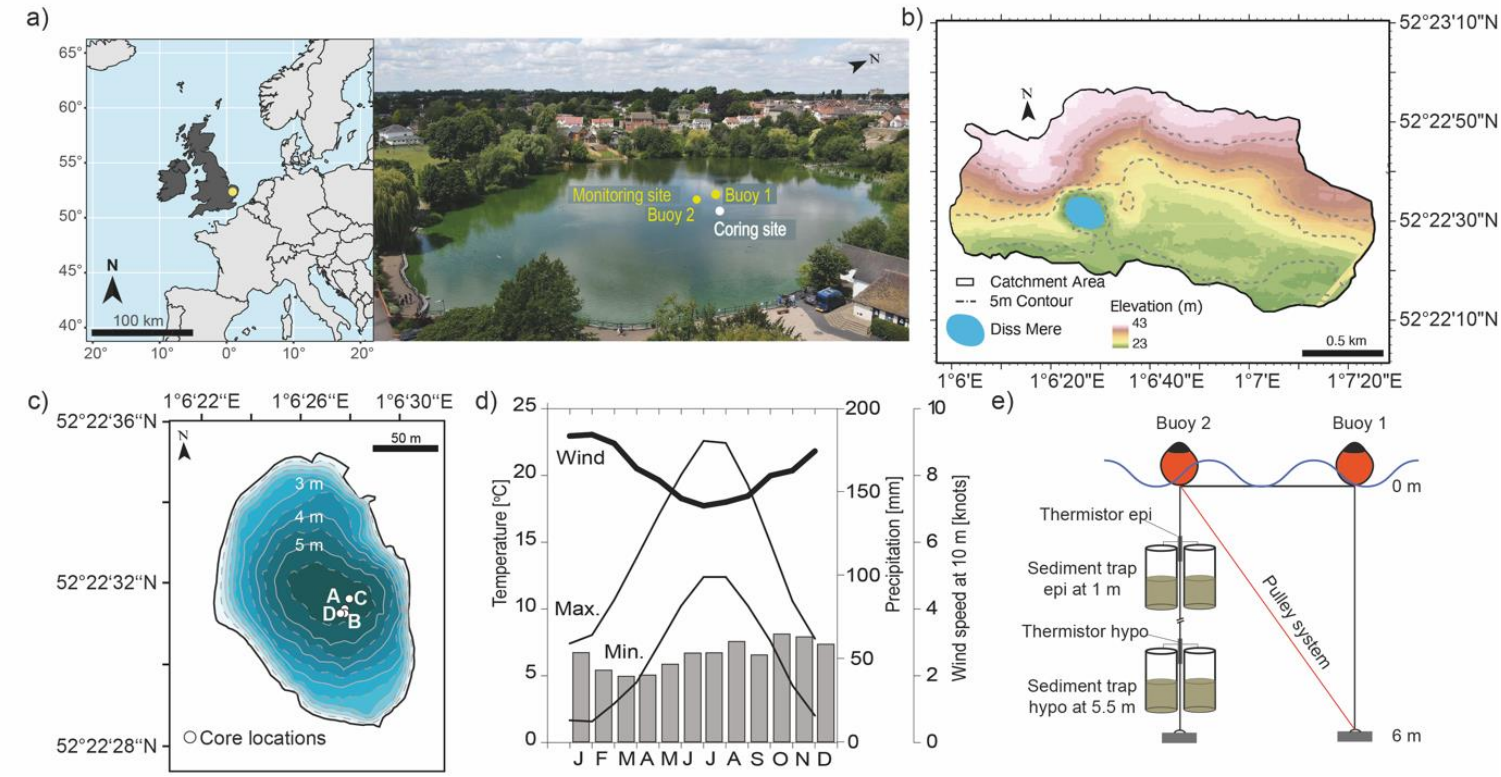

858 Figure 1. Settings of Diss Mere. a: geographical location and aerial photograph of the lake. b:
859 topography of the catchment area. c: Diss Mere bathymetry and core locations. d: climatograms
860 for East Anglia: maximum and minimum monthly temperature (thin black lines), monthly
861 precipitation (grey bars) and wind speed (thick black line). Data are monthly averaged between
862 1990-2020. Data source: Met Office at www.metoffice.gov.uk/research/climate/maps-and-
863 data/uk-climate-averages/u12cfksmy. e) diagram of the sediment traps based on a pulley
864 system. Epi is used for epilimnion and hypo for hypolimnion.
865
866
867
868
869
870

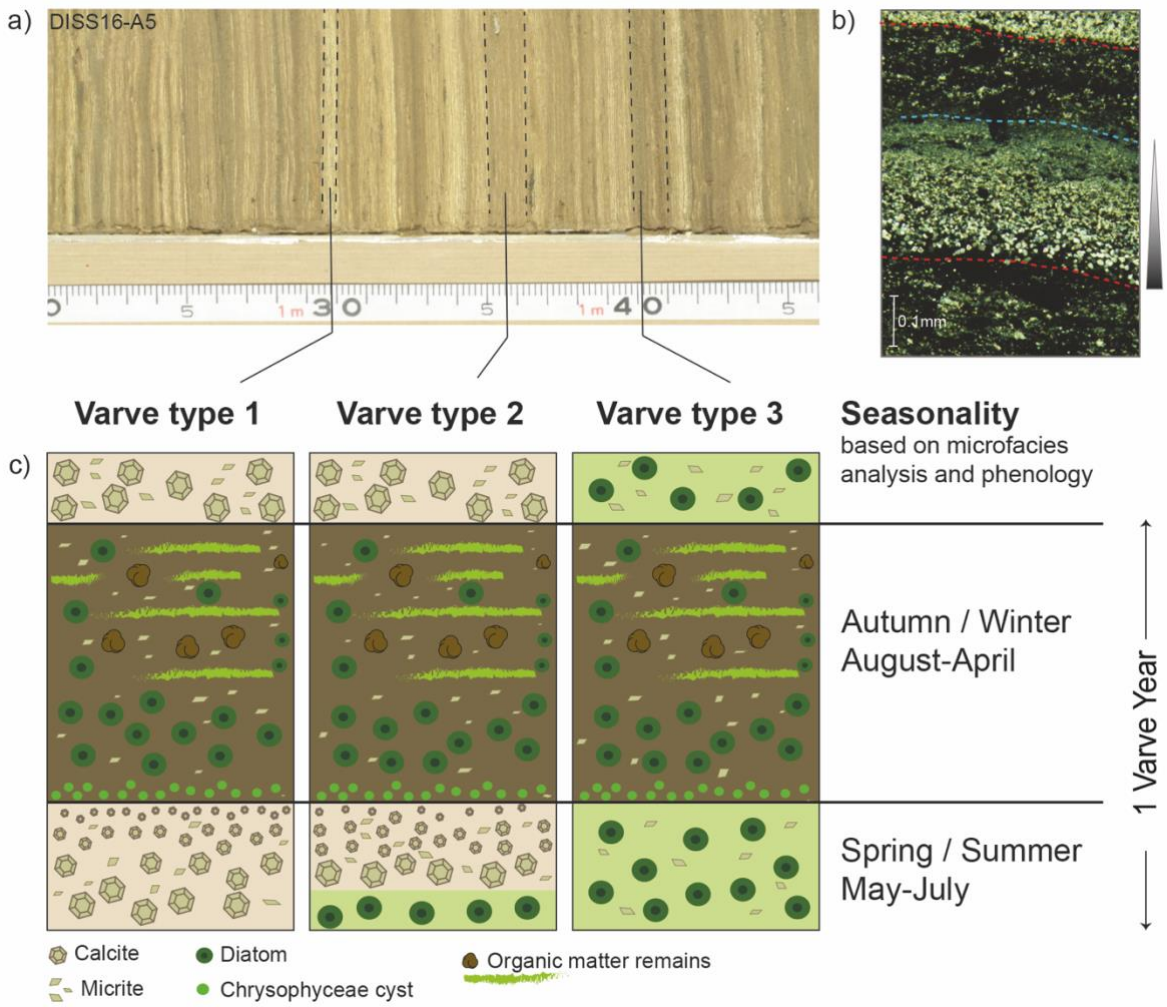

Figure 2. Diss Mere varve models. a: core photo section (DISS16-A5) of varved sediments showing interannual variability along the record as shown by the colour of the sediments. b: microscope image of a varve showing both the calcite (light) and the organic (dark) layers, and the gradient triangle depicts the gradually decreasing calcite grain size through the layer. c: model of the varve types identified in Diss Mere and their seasonality (Peglar et al. 1984; Martin-Puertas et al. 2021).

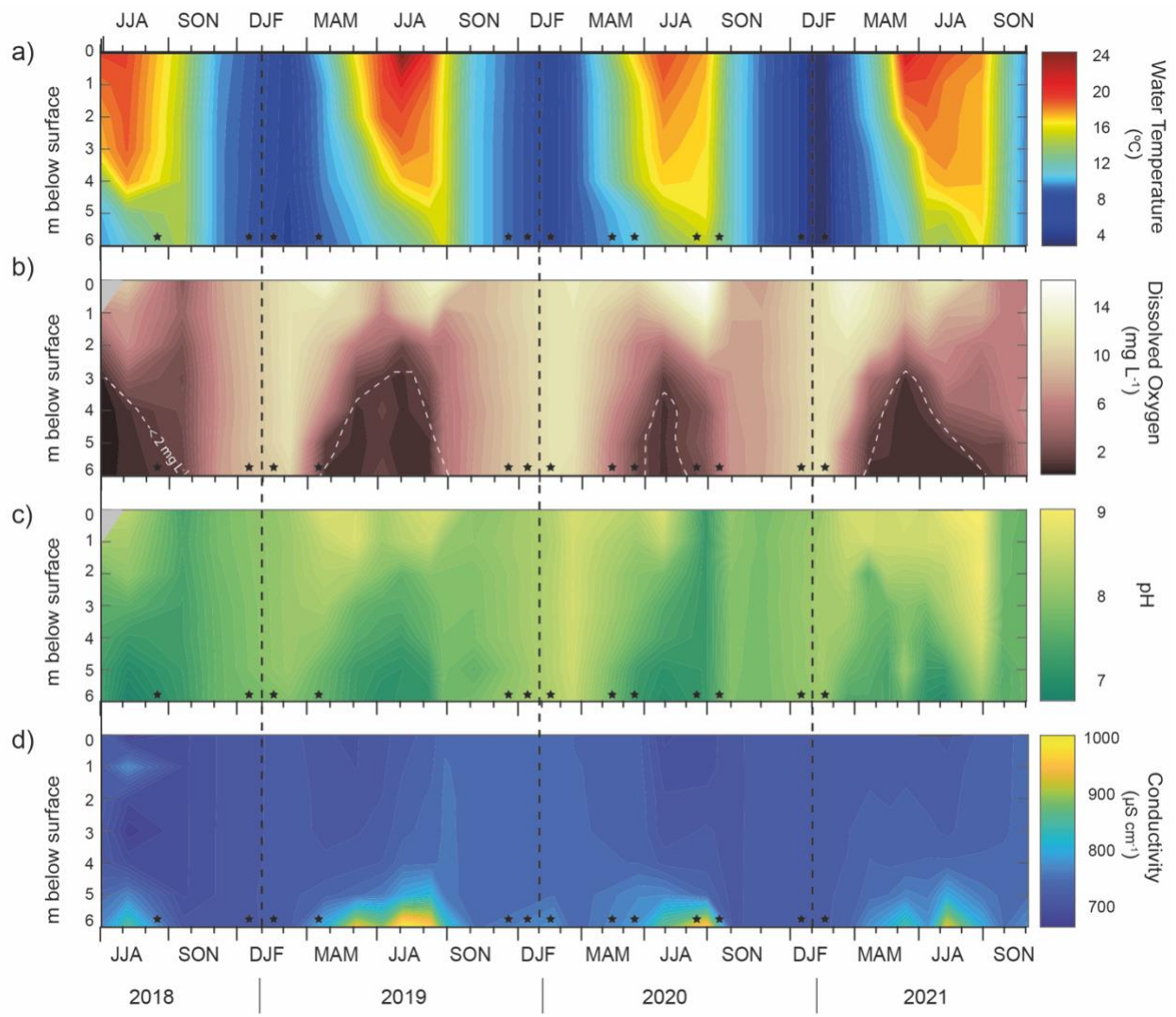

Figure 3. Contour plots of the main physical and chemical limnological variables in the water column over the monitored period (2018-2021). a: temperature. b: dissolved oxygen (DO) with white dashed line indicating the oxycline. c: pH; and d: electrical conductivity. Vertical black dashed lines indicate the beginning of a calendar year. Stars indicate months where data has been interpolated due to missing data. Grey triangles on b and c indicate that no data was collected for the surface water for this month.

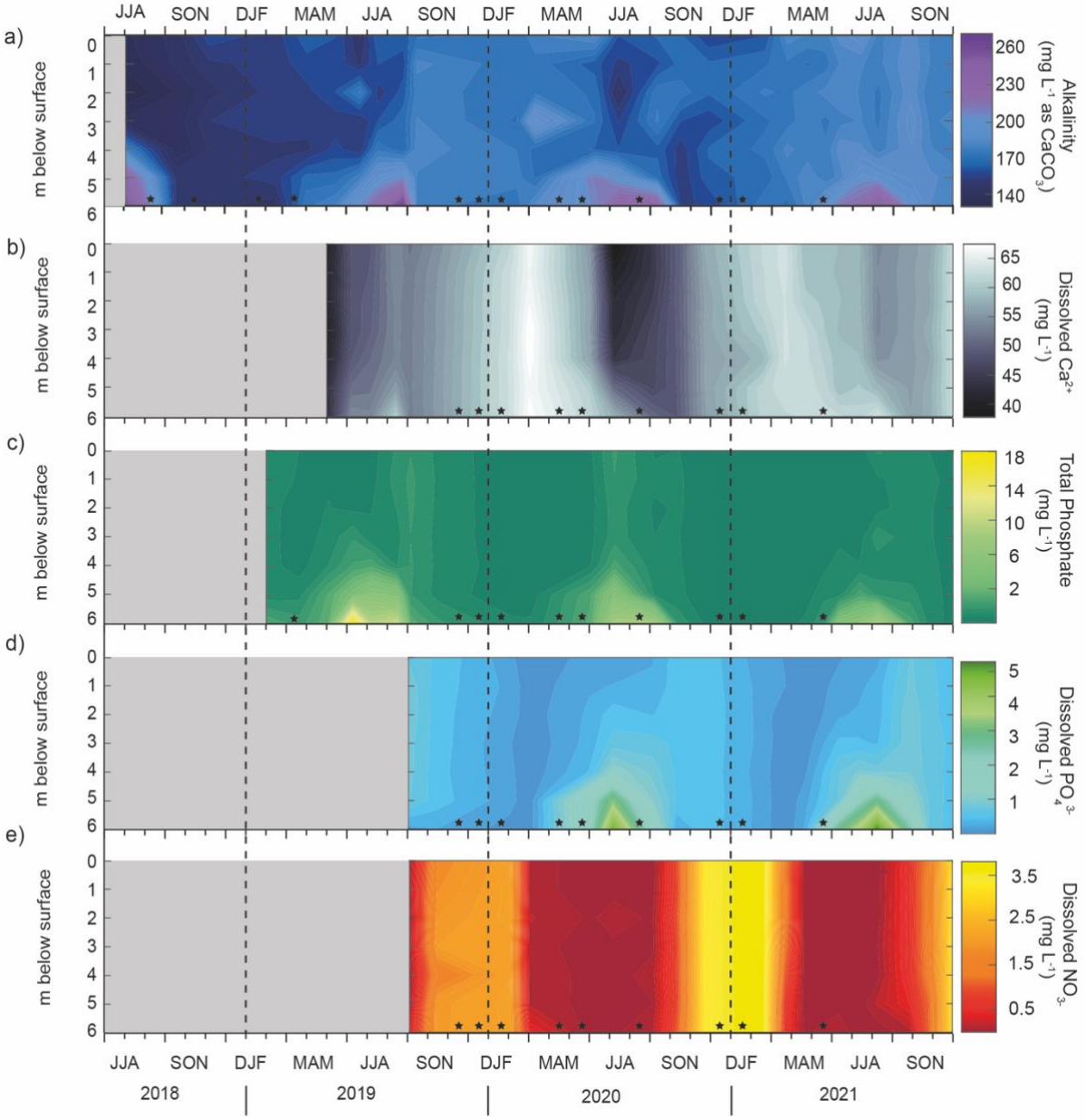

893 Figure 4. Chemical parameters for the monitored period (2018-2021). a: alkalinity. b dissolved
894 Ca^{2+}, c: total phosphate. d: dissolved PO_4^{3-} and e: dissolved NO^{3-}. Grey boxes indicate the
895 absence of data. Vertical black dashed lines indicate the beginning of a calendar year. Stars
896 indicate months where data has been interpolated due to absent data.

897

898

899

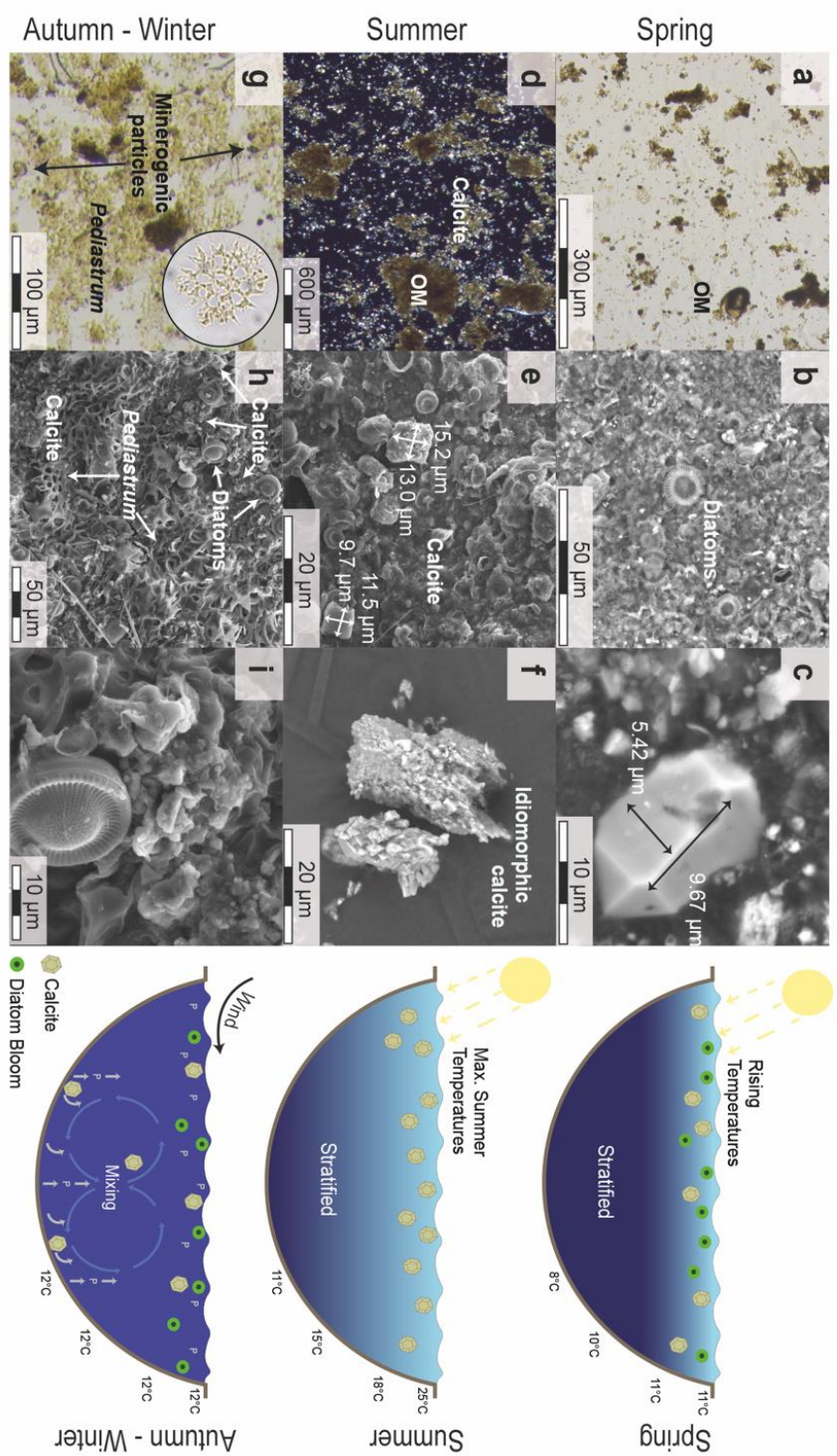

900 Figure 5. Dominant sediment composition and conceptual lake mixing and stratification cycle
901 for the different seasons at Diss Mere. Left panel a-i: smear slide images (a, d, g) and SEM
902 images (b, c, e, f, h, i) of the main components of the trapped material for each season. Right
903 panel: conceptual model for the annual lake mixing and stratification cycle.
904

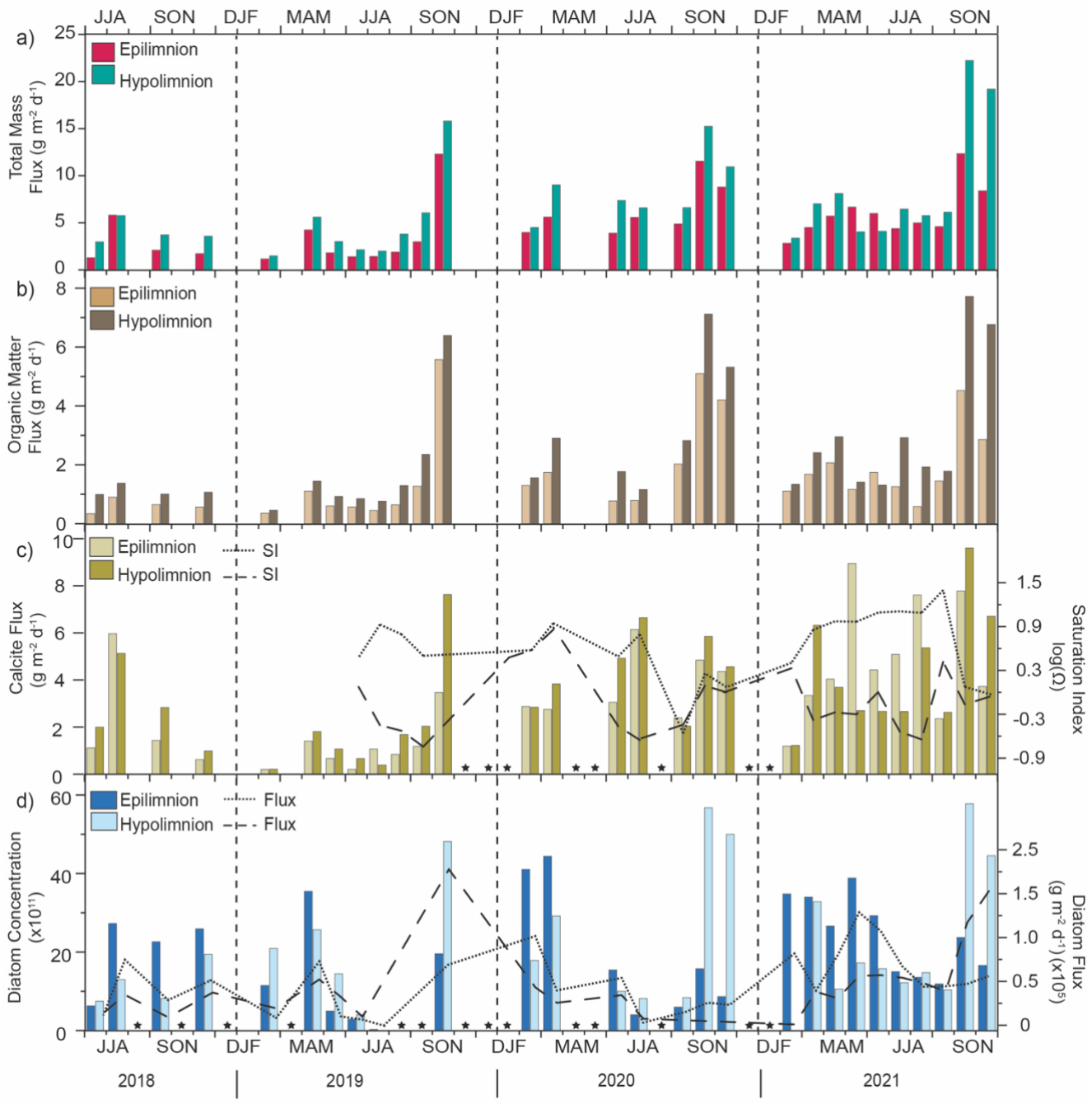

905 Figure 6. Flux and concentration data for the epi- and hypolimnion traps.

906 a: total mass flux. b: organic matter flux, c: calcite flux and saturation index (SI) (dashed lines).

907 d: diatom concentrations (bar graphs) and diatom fluxes (dashed lines). c and d contain stars to

908 indicate the months where data has been interpolated due to absent data Vertical black dashed

909 lines indicate the beginning of a calendar year.

910

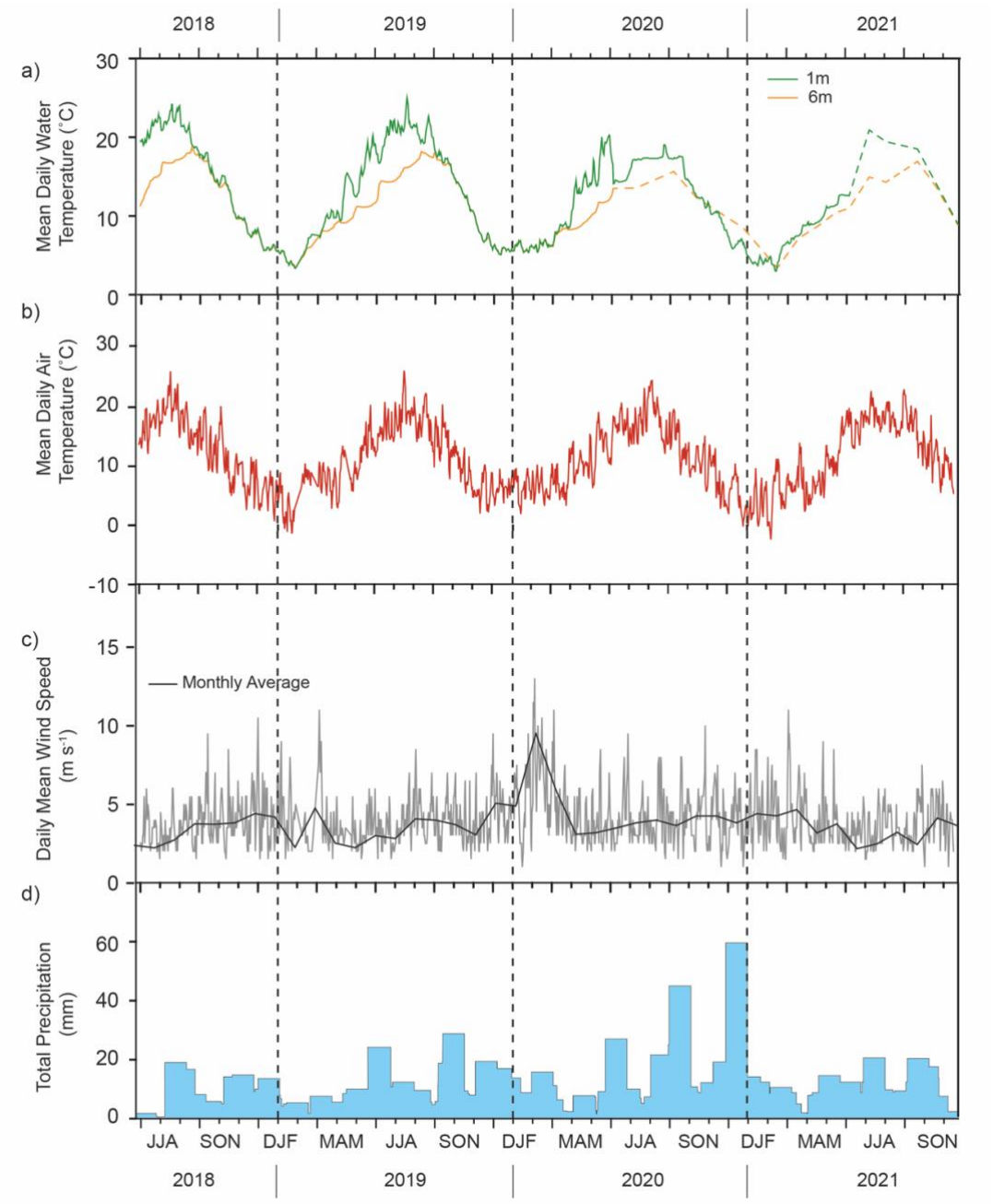

911 Figure 7. Thermistor timeseries from Diss Mere and meteorological information from the
912 Tibenham Airfield meteorological station between June 2018 and November 2021. a: water
913 temperatures recorded by the in situ thermistors at 1 m (green line) and 6 m (orange line) from
914 Diss Mere, calculated at daily mean intervals. Dashed line indicates when thermistors stopped
915 recording, and monthly temperature recordings are used in place. Stars indicate months where
916 temperature data has been interpolated due to absent data. b: daily mean air temperature. c:
917 daily mean wind speed (m s^{-1}) (grey line) and a monthly moving average (black line). d: total
918 daily precipitation (mm). Vertical black lines indicate the beginning of a new calendar year.